EUROFUSION WPS2-PR(15) 14480

WA Cooper et al.

Saturated ideal kink/peeling formations described as three-dimensional magnetohydrodynamic tokamak equilibrium states

Preprint of Paper to be submitted for publication in
Physics of Plasmas

This work has been carried out within the framework of the EUROfusion Consortium and has received funding from the Euratom research and training programme 2014-2018 under grant agreement No 633053. The views and opinions expressed herein do not necessarily reflect those of the European Commission.

A Three-Dimensional Magnetohydrodynamic Equilibrium Description of the Outer Mode/Edge Harmonic Oscillation in Quiescent H-Mode Tokamaks

W.A. Cooper, D. Brunetti, B.P. Duval, J.M. Faustin, J.P. Graves, A. Kleiner, H. Patten, D. Pfefferlé, L. Porte, M. Raghunathan, H. Reimerdes, O. Sauter, and T.M. Tran*
Ecole Polytechnique Fédérale de Lausanne (EPFL),
Centre de Recherches en Physique des Plasmas (CRPP), CH-1015 Lausanne, Switzerland
(Dated: September 8, 2015)

Abstract
Free boundary magnetohydrodynamic equilibrium states with spontaneous three dimensional deformations of the plasma-vacuum interface are computed for the first time. The structures obtained have the appearance of saturated ideal external kink/peeling modes. High edge pressure gradients yield toroidal mode number $n = 1$ corrugations for high edge bootstrap current and larger n distortions when this current is small. Deformations in the plasma boundary region induce a nonaxisymmetric Pfirsch-Schlüter current driving a field-aligned current ribbon consistent with reported experimental observations. A variation of the 3D equilibrium confirms that the $n = 1$ mode is a kink/peeling structure. We surmise that our calculated equilibrium structures constitute a viable model for the Edge Harmonic Oscillations and Outer Modes associated with quiescent H-mode operation in shaped tokamak plasmas.

1. Introduction

Tokamaks with high confinement operation (H-mode) [1] have a high edge pedestal pressure and sharp pressure gradient in the neighbourhood of the plasma boundary. The resulting plasma energy content is significantly higher than that of low confinement (L-mode) discharges. The economic feasibility of tokamak systems as reactor concepts is predicated on having a large $\langle\beta\rangle$ that is more readily achieved under H-mode, where $\langle\beta\rangle$ is the measure of the total thermal pressure over the confining magnetic pressure. As the pedestal grows, relaxation oscillations near the plasma boundary labelled Edge Localised Modes (ELM) develop [2]. Large amounts of energy expulsion ELMs generate would probably result in intolerable heat loads in a fusion reactor device. The Quiescent H-mode (QH) or a super H-mode can suppress ELMs and presents a possible path towards a tokamak fusion energy producing system [3].

Benign Edge Harmonic Oscillations (EHO) develop during QH-mode operation which can provide a mechanism for energy and impurity exhaust without the deleterious effects of ELMs [4]. The QH-mode lies at the kink/peeling edge of the peeling/ballooning stability boundaries predicted with the ELITE/EPED codes [5]. As another example, an Outer Mode (OM) in JET is associated with a long-lived quasistationary structure that suppresses ELMs [6] appearing to play a similar role to the EHO. Electron cyclotron emission measurements established that the OM is not due to a magnetic island [6]. Thus, the OM/EHO is likely to correspond to a saturated ideal kink driven mode as argued in Ref. [3]. On the TCV tokamak, nonlinear magnetic perturbations are dominated by low toroidal mode number n components in ELMy H-modes [7]. Finally, Quasicoherent mode structures were reported in QH mode AUG [8] and EAST [9] tokamak discharges that should be similar EHO and OM.

In this Letter, 3D free boundary ideal magnetohydrodynamic (MHD) equilibrium states are presented for the first time with the VMEC code [10] that develop significant edge distortions from a combination of large edge pressure gradient and the corresponding bootstrap current in simulations of TCV plasmas. We contend that the nonlinear saturated external ideal peeling/kink structures with low toroidal mode number n constitute the experimentally observed EHO and OM regimes. Additionally, we show that 3D distortions drive a nonaxisymmetric Pfirsch-Schlüter current component that induces a parallel current density ribbon. As the OM rotates toroidally at a frequency of $\sim 6kHz$ in JET [6], i.e., a very small fraction of an Alfvén time, simulations of these structures as static states constitute a fully valid approach.

2. 3D equilibria as saturated nonlinear ideal MHD states

Computation of 3D MHD equilibrium states is based on the VMEC code [10] that imposes nested magnetic flux surfaces. The plasma energy $\mu_0 W = \int\int\int d^3x[B^2/2 + p(s)/(\Gamma - 1)]$, where $\boldsymbol{B}$ is the magnetic field, $p(s)$ is the plasma pressure and is a function of the radial variable s ($0 \leq s \leq 1$) which is proportional to the enclosed toroidal magnetic flux function Φ, and Γ, the adiabatic index. This is minimised with respect to an artificial time variable employing a steepest descent energy minimisation scheme. A Green's function technique is applied to evolve the plasma-vacuum interface to obtain free boundary MHD equilibria where the vacuum magnetic fields are calculated using Biot-Savart's Law from all toroidal and poloidal field coils discretised into finite sized filaments.

We apply the code to compute free boundary TCV-like

equilibria. Up-down symmetry is imposed with $N_s = 289$ radial grid points and a poloidal $0 \leq m \leq 10$ and toroidal $-6 \leq n \leq 6$ mode spectrum. The poloidal mode numbers were extended to m to 14 for a limited set of calculations. We undertake a scoping study by independently varying the edge pressure gradient p' and the total integrated bootstrap current J_{BS}. As J_{BS} depends on the pressure and the density and the collisionality of the plasma, we retain a margin of manoeuvring space for consistency between p' and J_{BS}. A set of 3 TCV configurations was examined with fixed total toroidal current $I_t = 340kA$, volume averaged $\langle\beta\rangle \sim 1.9\%$ and $\beta_N \sim 2.5$. The toroidal current profile $\langle \boldsymbol{j} \cdot \boldsymbol{\nabla} v \rangle$ (where $\langle A \rangle$ constitutes the flux surface average of A and v is the label of the toroidal angle) and the pressure profile $p(s)$ were varied. The prescribed pressure and the toroidal current profiles are shown together with the corresponding q-profiles on the top row of Fig. 1 for a case with $(p' < 0; J_{BS} > 0)$, $(p' < 0; J_{BS} \sim 0)$ and $(p' \sim 0; J_{BS} \sim 0)$ near the edge. The current profile for the case with $J_{BS} > 0$ corresponds a hybrid/advanced scenario operation (reversed central shear with minimum value of q greater than unity). The shapes of the last closed magnetic flux contour at 4 different toroidal angle cross sections spanning half a toroidal transit are presented on the middle row of Fig. 1. For edge $(p' < 0; J_{BS} > 0)$, toroidal mode number $n = 1$ corrugations dominate. For edge $(p' < 0; J_{BS} \sim 0)$, $n = 4$ boundary distortions dominate. Finally, for edge $(p' \sim 0; J_{BS} \sim 0)$, characteristic of L-mode type discharges, the deformation has mainly $n = 4$ components but of much smaller magnitude than the $(p' < 0; J_{BS} \sim 0)$ case. We next examine the axisymmetry breaking Fourier spectrum of B on the last closed magnetic flux surface. The Fourier components B_{mn} as a function of the poloidal mode number m with toroidal mode number n are displayed on the bottom row of Fig. 1 for the equilibria. Equilibria with edge $(p' < 0; J_{BS} > 0)$ show dominant $n = 1$ components attaining $0.02T$ for $m/n = 2/1$ and there are subdominant contributions with $n = 2$, 3 and 4. Edge $(p' < 0; J_{BS} \sim 0)$ has dominant $n = 4$ Fourier components with $m = 6$ displaying a maximum of $0.01T$. Finally, the L-mode case, edge $(p' \sim 0; J_{BS} \sim 0)$, displays a similar spectrum structure to that of the edge $(p' < 0; J_{BS} \sim 0)$, but with 1/3 the magnitude.

Fig. 1 demonstrates that an edge pressure gradient enhances the boundary deformation and the edge bootstrap current tends to suppress the edge corrugation for toroidal mode numbers $n > 1$, while significantly amplifying the $n = 1$ distortions. Large edge $p' < 0$ destabilises external ideal MHD modes that can saturate. When the edge $J_{BS} \sim 0$ (i.e., at high collisionality), the saturated mode structures are dominantly $n = 4$, with $2 \leq m \leq 8$ that are indicative of ballooning character. When the edge $J_{BS} > 0$, the saturated structures are kink/peeling type with $m/n = 2/1$, $4/1$, $5/1$ and $1/1$ main components. These $n = 1$ saturated structures are a valid model to describe the EHO/OM observed in QH-mode tokamak operation. Alhough the plasma boundary is 3D distorted, the central region of the plasma remains axisymmetric. In TCV simulations, the plasma boundary corrugation, caused by the saturated ideal external kink, develops when $\langle\beta\rangle > 1.2\%$.

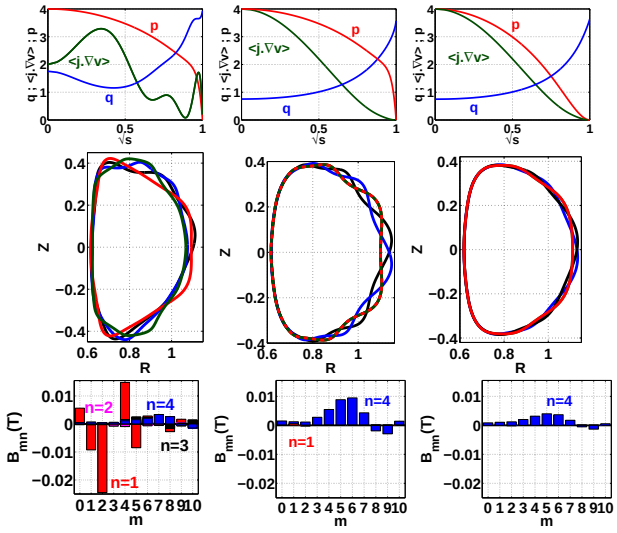

FIG. 1. (Top row) the pressure, toroidal current and q-profiles in TCV at $\langle\beta\rangle = 1.89\%$, $\beta_N \sim 2.47$, with toroidal current $I_t = 340kA$ and toroidal magnetic field $B_t = 1.43T$ at $R = 0.8m$ in 3 configurations for large and small edge pressure gradients and bootstrap currents. (Middle row) the shape of the last closed magnetic flux surface at toroidal angles $v = 0, \pi/3, 2\pi/3$ and π projected on a single plane for the profiles shown on the top row i.e. large edge $(p' < 0; J_{BS} > 0)$ (left), edge $(p' < 0; J_{BS} \sim 0)$ (middle) and edge $(p' \sim 0; J_{BS} \sim 0)$ (right). (Bottom row) dominant Fourier amplitudes of the magnetic field B components that break axisymmetry $(n \neq 0)$ at the last closed magnetic flux surface as a function of the poloidal mode number m for toroidal mode numbers $n = 1$, 2, 3 and 4 for the same profiles.

The operating domain for 3D equilibrium states at fixed $\langle\beta\rangle = 1.9\%$ and toroidal current $I_t = 375kA$ in TCV is computed in Fig. 2 in the space of the ratio of the bootstrap current to the total current J_{BS}/I_t as a function of the pressure gradient evaluated at the radial position $s = 0.948$ (the position of the peak in the edge bootstrap current profile). The domain is extended by enhancing the mix between the edge localised bootstrap and the peaked Ohmic current profiles and altering the shape of the pressure profile from peaked to slighty hollow to scan of the abscissa. The upper boundary corresponds to the kink/peeling limit and the lower right boundary is defined by the peeling/ballooning limit originally identified with ELITE calculations [11]. Black diamond shaped symbols indicate converged 3D MHD equilibrium states where the dominant symmetry breaking Fourier ampli-

tudes of B have toroidal mode number $n = 4$ and blue circles where the $n = 1$ components of B dominate. These correspond to cases where J_{BS}/I_t typically exceeds 30% and trace the domain where kink/peeling structures describe the distortion of the plasma boundary shape. The domain for which the $n = 4$ Fourier amplitudes of B are most significant are, in our consideration, indicative of the high n peeling/ballooning boundary. Red squares represent unconverged states indicative of a plasma that is so unstable to kink/peeling/ballooning modes that experimental operation beyond this boundary is strongly susceptible to ELMs.

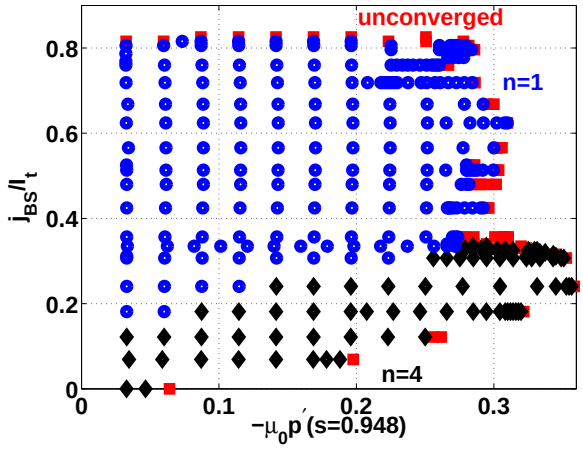

FIG. 2. The operating domain at fixed $\langle\beta\rangle = 1.9\%$ and toroidal current $I_t = 375kA$ of the variation of J_{BS}/I_t (edge bootstrap to total current ratio) versus pressure gradient. Blue circles, black diamonds and red squares correspond to 3D MHD equilibrium states with plasma boundary dominant symmetry breaking Fourier amplitude of B of toroidal mode number $n = 1$, $n = 4$ and unconverged states, respectively. Here $p' \equiv dp/d\Phi$.

Turning to JET, the Outer Mode (OM) is described by a field-aligned helical current ribbon [6]. Crucially, our computed 3D MHD equilibrium recovers this filamentary current structure as shown in Fig. 3. The structures we ontain are driven by the Pfirsch-Schlüter current. As this is proportional to the pressure gradient, it is never fully clear whether the mode is driven by the current or the pressure gradient [12]. The distribution of $\sqrt{g}(\mu_0 j_{||})^2$ on a toroidal flux surface with $\sqrt{s} \simeq 0.95$ is on the figure left and the profiles in the edge region of the leading Fourier amplitudes of the parallel current density factor $j_{||}/B$ are on the right. The $\sqrt{g}(\mu_0 j_{||})^2$ distribution is dominated by a $m = 3, n = 1$ component and the $m = 0, n = 0$ Fourier component of $j_{||}/B$ corresponds to the edge bootstrap current contribution. Force balance and charge conservation mean that the Pfirsch-Schlüter current drives the surface varying components of $j_{||}$, in particular, the $m = 3, n = 1$ component of $j_{||}/B$ that describes a field-aligned ribbon similar to the JET report [6]. A $m = 6, n = 2$ component appears and the next largest is $m = 13, n = 4$ (not shown to simplify the figure) that are consistent with the rich harmonic spectrum described in Ref. [6]. It is our opinion that the EHO in DIII-D and the OM in JET result from the same physical phenomenon so a helical current density pattern should emerge when an EHO is detected. For configurations with lower edge bootstrap current that display dominant $n = 4$ boundary distortions, the helical parallel current pattern compresses radially from a ribbon to a sheet.

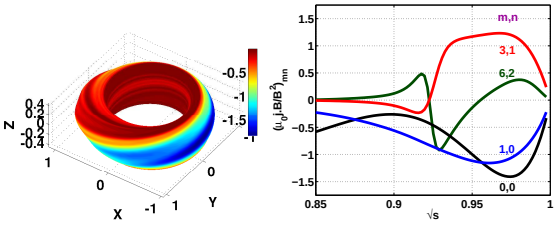

FIG. 3. Distribution of $\sqrt{g}(\mu_0 j_{||})^2$ on a toroidal flux surface $\sqrt{s} \simeq 0.95$ (left) and profiles of the leading Fourier amplitudes of the parallel current density $j_{||}/B$ from $\sqrt{s} = 0.85$ to 1 (right) for a TCV configuration with large edge bootstrap current $J_{BS}/I_t = 0.5658$, volume averaged $\langle\beta\rangle = 1.9\%$, $I_t = 375kA$. The Jacobian of the transformation from Cartesian to Boozer coordinates is denoted by $\sqrt{g}$ [13].

A second variation of the plasma energy functional yields the linear ideal MHD energy principle where the amplitude of the instability driving term is conveniently expressed as $D = D_B + D_K$ [14–16], composed of a ballooning term involving the interaction of the pressure gradient with the magnetic field line curvature, namely $D_B = 2p'(s)\boldsymbol{\kappa} \cdot \boldsymbol{\nabla} s$, and a kink term describing the interaction of the parallel current density with the local magnetic shear, namely $D_K = \sigma(S|\boldsymbol{\nabla} s|^2 + \sigma B^2)$. The magnetic field line curvature is $\boldsymbol{\kappa} = (\boldsymbol{b} \cdot \boldsymbol{\nabla})\boldsymbol{b}$ with $\boldsymbol{b} = \boldsymbol{B}/B$ the unit vector along the magnetic field lines, while the local magnetic shear is $S = -\boldsymbol{h} \cdot \boldsymbol{\nabla} \times \boldsymbol{h}$ with $\boldsymbol{h} = \boldsymbol{B} \times \boldsymbol{\nabla} s/|\boldsymbol{\nabla} s|^2$. The parallel current density factor is $\sigma \equiv \boldsymbol{j} \cdot \boldsymbol{B}/B^2 = j_{||}/B$. Ideal linear MHD stability calculations for the eigenvalue and eigenfunction are surplanted by the diagnostic routines of the TERPSICHORE code [17, 18] to evaluate the instability drive terms [16] in Boozer magnetic coordinates [13] with poloidal angle θ and toroidal angle ϕ. The top row of Fig. 4 shows interactions of the pressure gradient with the magnetic field line curvature and the parallel current density with the local magnetic shear on an unwrapped toroidal magnetic flux contour with $s \sim 0.974$ near the edge of the plasma in TCV for the H-mode like plasma, $(p' < 0; J_{BS} > 0)$. The destabilising ballooning drive $2\sqrt{g}p'(s)\boldsymbol{\kappa} \cdot \boldsymbol{\nabla} s$ term is ~ 3 smaller than the kink/peeling term $\sqrt{g}\sigma(S|\boldsymbol{\nabla} s|^2 + \sigma B^2)$ that also has a strong $n = 1$ modulation at toroidal angle $\phi \sim \pi$ at the

outer edge of the plasma. $\sqrt{g}\sigma^2 B^2$ dominates the kink drive, implying that the parallel current term $j_{||}^2/B^2$ is the main source of energy for the MHD instability in linear theory. In contrast, the L-mode equilibrium state with edge ($p' \sim 0; J_{BS} \sim 0$), presented in the bottom row of Fig. 4, shows ballooning kink drive terms of comparable magnitude with a dominant $n = 4$ structure near the outer edge of the plasma. $\sigma S|\nabla s|^2$ is an order of magnitude larger than the other component of the kink/peeling drive. Linear ideal MHD stability analyses with the TERPSICHORE code [17, 18] of the axisymmetric limit of selected 3D equilibria we have obtained are consistent with the saturated nonlinear states calculated with the VMEC code, particularly when we take into account the evolution of dominant unstable large n toroidal mode numbers in the linear phase to $n \approx 1$ structures in the nonlinear phase that has been previously reported [7, 19, 20].

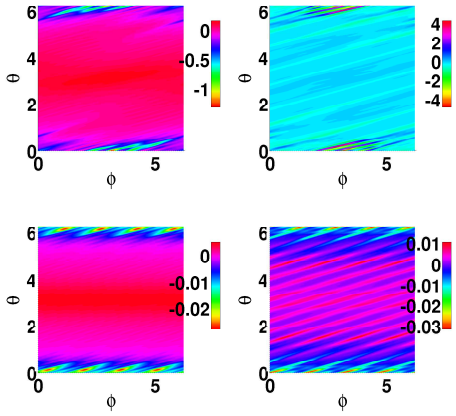

FIG. 4. Interaction of the pressure gradient with the magnetic field line curvature $2\sqrt{g}p'(s)\boldsymbol{\kappa}\cdot\nabla s$ (left) and the interaction of the parallel current density with the local magnetic shear $\sqrt{g}\sigma(S|\nabla s|^2 + \sigma B^2)$ (right) on an unwrapped toroidal magnetic flux surface at $s \sim 0.974$ for the H-mode TCV case with large edge ($p' < 0; J_{BS} > 0$) (top row, corresponding to the far left column of Fig. 1) and for the L-mode TCV case with vanishing edge ($p' \sim 0; J_{BS} \sim 0$) (bottom row, corresponding to the far right column of Fig. 1).

3. Summary and Conclusions

We report, for the first time, free boundary tokamak equilibria using the VMEC code with novel spontaneously developed unprompted 3D distortions to the plasma-vacuum interface when $\langle\beta\rangle$ exceeds a threshold value. Corrugations are predicted to occur for $\langle\beta\rangle > 1.2\%$ in the TCV tokamak. Solutions with 3D deformations are shown to resemble saturated nonlinear ideal kink/peeling instability structures. For H-mode type plasmas, displaying a significant edge $p' < 0$, the dominant symmetry breaking equilibrium structures have toroidal mode number $n = 1$ when the edge bootstrap current is large and $n = 4$ when this current becomes small. Our calculations are limited to poloidal mode numbers m to 14 and toroidal mode numbers n to ± 6 which is sufficient only to rigourously resolve low-n corrugations, but not nonlinearly saturated ballooning modes. Configurations for which $n = 1$ symmetry-breaking components of B dominate are identified as corresponding to equilibrium states that model the EHO/OM confirming the speculation in Ref. [3] that the EHO is the saturated state of a current-driven mode. Configurations for which $n = 4$ symmetry-breaking components of B at the edge are largest constitute, in our opinion, indications of equilibrium states that are susceptible to higher$n$ peeling/ballooning destabilisation, which we are not able to resolve. The I-mode, reported on C-mod, represents another quiescent structure of reactor relevance, but with typical mode numbers of the weakly coherent mode observed [21] that are higher than those we have resolved in our nonlinear equilibrium computations. This work does, however, not exclude a similar 3D explanation for the I-mode. The 3D deformation of the plasma boundary region drives nonaxisymmetric components of the Pfirsch-Schlüter current that induce a field-aligned helical current ribbon that reproduces the OM in JET [6]. Linear MHD stability analyses confirm the structure of nonlinearly saturated states computed with the equilibrium solver from which we have further identified the Pfirsch-Schlüter current as playing an important role as an instability driving mechanism.

We contend that the 3D edge structures we compute serve as a model for the benign Edge Harmonic Oscillations (EHO) and the Outer Mode (OM) that are observed during Quiescent H-mode operation reported from DIII-D, JET, AUG and other tokamaks. We have naturally captured the nonlinear amplitudes and mode component interactions using an equilibrium solver to model the experimental modulations that are absent in linear stability calculations to determine the kink/peeling/ballooning boundaries. The Quiescent H-mode equilibrium states obtained provide a solid basis for investigating tokamak physics phenomena that encompass a broad range of fields including fast particle confinement, bootstrap current, neoclassical and turbulent transport, heating and current drive, edge physics and control mechanisms to model the operational limits of tokamaks in high $\langle\beta\rangle$ advanced scenarios. The economic feasibility of tokamak reactor, conceived today, require H-mode scenarios. However, as this mode is unsustainable if Edge Localised Modes are triggered, Quiescent H or Super H present a viable operational regime [3].

Acknowledgments

This work has been carried out within the framework

of the EUROfusion Consortium and has received funding from the European Union's Horizon 2020 research and innovation programme under grant agreement number 633053. The views and opinions expressed herein do not necessarily reflect those of the European Commission. The project was also supported in part by the Swiss National Science Foundation. We thank Dr. S. P. Hirshman for providing us with the VMEC code and acknowledge fruitful discussions with M. Becoulet, R. Buttery, A. Garofalo, C. Paz-Soldan, P. Snyder, E. Solano, W. Solomon, F. Turco, A. Turnbull and H. Wilson. Much of the numerical work was performed at the CSCS, Lugano, Switzerland, at the Helios and CADMOS platforms.

* wilfred.cooper@epfl.ch

References

[1] F. Wagner *et al.*, Phys. Rev. Lett. **49**, 1408 (1982).
[2] H. Zohm, Plasma Phys. Control. Fusion **38**, 105 (1996).
[3] W.M. Solomon *et al.*, Phys. Rev. Lett. **113**, 135001 (2014).
[4] K.H. Burrell *et al.*, Phys. Plasmas **12**, 056121 (2005).
[5] P.B. Snyder *et al.*, Phys. Plasmas **16**, 056118 (2009).
[6] E.R. Solano *et al.*, Phys. Rev. Lett. **104**, 185003 (2010).
[7] R.P. Wenninger, H. Reimerdes, O. Sauter and H. Zohm, Nucl. Fusion **53**, 113004 (2013).
[8] W. Suttrop *et al.*, Nucl. Fusion **45**, 721 (2005).
[9] J.S. Hu *et al.*, Phys. Rev. Lett. **114**, 055001 (2015).
[10] S.P. Hirshman, W.I. van Rij and P. Merkel, Comput. Phys. Commun. **43**, 143 (1986).
[11] P.B. Snyder, H.R. Wilson and X.Q. Qu, Phys. Plasmas **12**, 056115 (2005).
[12] A.D. Turnbull, M.A. Secrétan, F. Troyon, S. Semenzato and R. Gruber, J. Comput. Phys. **66**, 391 (1986).
[13] A.H. Boozer, Phys. Fluids **23**, 904 (1980).
[14] R.L. Dewar *et al.*, Phys. Fluids **27**, 1723 (1984).
[15] J.M. Greene, Phys. Plasmas **3**, 8 (1996).
[16] W.A. Cooper, Phys. Plasmas **4**, 153 (1997).
[17] D.V. Anderson *et al.*, Int. J. Supercomp. Appl. **4**, 34 (1990).
[18] W.A. Cooper, Plasma Phys. Control. Fusion **34**, 1011 (1992).
[19] I. Krebs, M. Hölzl, K. Lackner and S. Günter, Phys. Plasmas **20**, 082506 (2013).
[20] F. Liu, G. T. A. Huijsmans, A. Loarte, A. M. Garofalo, W. M. Solomon, P. B. Snyder, M. Hoelzl and L. Zeng, Nucl. Fusion **55**, 11302 (2015).
[21] D.G. Whyte *et al.*, Nucl. Fusion **50**, 105005 (2010).